

# Monte Carlo Calculations of Neutron Penetration through Graphite and Polyethylene at Energies of 30 and 45 MeV.

By

Yositomo UWAMINO, Kazuo SHIN, Mistuo YOSHIDA\*,  
and Tomonori HYODO

(Received December 25, 1978)

## Abstract

A new Monte Carlo code was developed to calculate neutron penetration through graphite and hydrocarbon. The accuracy of the code was checked with the experimental values. Attenuation profiles of 30 and 45 MeV monoenergetic neutrons through graphite and polyethylene slabs were obtained by the Monte Carlo calculation. Macroscopic removal cross sections were calculated from the profiles.

## I. Introduction

Knowledge of neutron penetration through materials in the energy range 10–30 MeV is very important for an accelerator shielding design, because neutrons in this energy range are predominant even in higher-energy accelerators. A few papers<sup>1)–4)</sup> were published about neutron attenuation measurements with energy higher than 15 MeV. Attenuation profiles of mono-energetic neutrons above 15 MeV were not obtained, because the monochromatic-neutron source of this energy is hardly available.

Alsmiller et al.<sup>5)–7)</sup> calculated the mono-energetic neutron transport through concrete with energies up to 400 MeV, using the discrete-ordinate transport codes, ANISN<sup>5),6)</sup> and DOT<sup>6)</sup>. In their calculations, non-elastic cross sections above 15 MeV taken from the analytic fittings<sup>8)</sup> to the theoretical data given by Bertini<sup>9)</sup>. Bertini's results, however, are not so accurate in the energy range below 50 MeV, which was shown experimentally by Nakamura et al.<sup>10)</sup> and Faso et al.<sup>11)</sup>.

We developed a Monte Carlo code to calculate neutron penetration through graphite and hydrocarbon, because these materials are generally used in an accelerator shield.

\* Department of Nuclear Engineering

\*\* Present address: Nippon Steel Co. Ltd., 5-3 Tokai-cho, Tokai-shi, Aichi-ken

Cross sections used in this code were based on experimental data. The code was already applied<sup>1)</sup> successfully to neutron penetration problems through graphite shields, using neutrons from a carbon target irradiated by 52-MeV protons as source neutrons.

Neutron attenuation profiles in graphite and polyethylene slabs were studied by this code for the mono-energetic neutrons of 30 and 45 MeV. This paper is intended to report the details of the code and the calculated results for the mono-energetic neutron penetration.

## II. Description of Monte Carlo Code

A Monte Carlo code was developed for neutron transport calculation through graphite and hydrocarbon based on the Monte Carlo codes, CYGNUS<sup>12)</sup> and O5S<sup>13)</sup>. Neutron energies below 50 MeV were expected in the calculation.

### 1) Treatments of Neutron Reactions

Most of the neutron reactions occurred in the media were handled by the treatments based on the O5S code. The detailed descriptions of the neutron-reaction treatments are given here.

#### (i) Nuclear Reactions with Carbon Nucleus

The following reactions with a carbon nucleus were considered in the calculation: absorption,  $(n, n)$ ,  $(n, n')$ ,  $(n, n'3\alpha)$ ,  $(n, pn)$  and  $(n, 2n)$  reactions. The absorption contained  $(n, \alpha)$  and  $(n, p)$  reactions, from whose reactions no neutron emerged. References from which the cross section data were quoted are shown in Table 1. The total cross sections and cross section data for  $(n, n)$  and  $(n, n')$  reactions were taken from the KFK-750<sup>14)</sup> data file for energies lower than 10 MeV, from the ENDF/B-III<sup>15)</sup> file for energies 10–14 MeV and from the O5S library data file for the energy range above 14 MeV. Cross sections for all other reactions were taken from the O5S data.

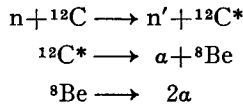
The sixth order Legendre expansion was used to represent the anisotropy of the angular distribution of elastically scattered neutrons. The Legendre coefficients in the expansion were taken from the O5R<sup>16)</sup> library data as shown in Table 1. Because the sixth order expansion was not enough to express the strongly forward-peaked angular distribution, the distribution function became negative at certain large angles, when the neutron energy was higher than 11.3 MeV. In this work, however, the attenuation profiles of integral values such as dose equivalent and total flux were considered. This effect did not affect the calculated results, because the forward-scattered neutrons were always predominant behind the shield.

In the inelastic scattering,  $(n, n')$ , only the first and the second excited levels were considered. The excitation functions for these levels were obtained from the KFK-750 file for energies lower than 10 MeV. The data at 10 MeV were utilized for energies higher than 10 MeV. In the  $(n, n'3\alpha)$  reaction, the carbon nucleus was excited at first

Table 1. References of Cross Sections Used in the Monte Carlo Calculation.

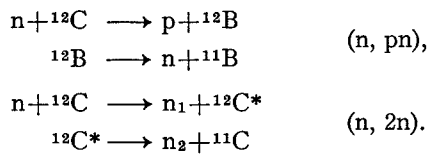
Nuclide	Type	Reference	Energy Range (MeV)
Hydrogen ( $^1_1\text{H}$ )	$\sigma_{\text{total}}$	ENDF/B-III	0 - 14
		O5S library	14 - 45
	$d\sigma/d\Omega$	O5S library	
Carbon ( $^{12}_6\text{C}$ )	$\sigma_{\text{total}}$	KFK-750	0 - 10
		ENDF/B-III	10 - 14
		O5S library	14 - 45
	$\sigma_{\text{el.}}$	KFK-750	0 - 10
		ENDF/B-III	10 - 14
		O5S library	14 - 45
	$d\sigma/d\Omega$	O5R library	
	$\sigma_{\text{inel.}}$	KFK-750	0 - 10
ENDF/B-III		10 - 14	
O5S library		14 - 45	
$\sigma_{\text{n } n^{3\alpha}}$	O5R library O5S library	0 - 14 14 - 45	
$\sigma_{\text{n } p\text{n}}$	O5S library		
$\sigma_{\text{n } 2\text{n}}$	O5S library		

by the inelastic collision with the neutron, then the residual nucleus decayed to three  $\alpha$  particles. This is shown by the reaction scheme:



Four excited levels, from the second to the fifth state of carbon nucleus, were considered in the calculation of the scattered neutron energy, using the excitation functions quoted from the O5S code. Scattering angles of the neutron from the (n, n') and (n, n'3 $\alpha$ ) reactions were sampled from the isotropic distribution in the center-of-mass (C-M) coordinates.

The reaction schemes of the (n, pn) and (n, 2n) reactions are shown as follows:



Energies of all outgoing neutrons from these reactions were calculated from the energy-

distribution functions derived from the evaporation model:

$$\Phi(E) = E \cdot \exp[-E/T],$$

$$(0 \leq E \leq E_{\max}),$$

where  $E$  is the neutron energy,  $T$  is the nuclear temperature<sup>13)</sup>, and  $E_{\max}$  is the maximum energy determined from Q-values<sup>13)</sup> of the reactions.

The center of mass polar angle of the first outgoing neutron from (n, 2n) reaction was calculated from

$$p(\theta) = \left(2 - \frac{1}{\pi} \theta\right) \sin \theta$$

over the interval  $(0, \pi)$ . The other neutrons from these reactions were assumed to be emitted isotropically in the C-M system. The (n, 2n) reaction was supposed to occur only once at most in one history for the sake of simplicity.

Neutron emitting reactions which could be induced by charged particles, generated in the neutron reactions in the media, were completely omitted from the calculation, because the contribution from these cascade reactions was very small in the energy range considered here.

#### (ii) Nuclear Reactions with Hydrogen

The neutron reaction with hydrogen was regarded as elastic scattering only, and the (n,  $\gamma$ ) reaction was ignored, because a lower cutoff energy of the Monte Carlo calculation was kept at 50 keV and the (n,  $\gamma$ ) reaction of hydrogen can be ignored completely. The cross-section data for the elastic collision were quoted from the ENDF/B-III file in the energy range lower than 14 MeV, and from the O5S data library for energies above 14 MeV, as shown in Table 1. The angular distribution of scattered neutrons became slightly anisotropic in the C-M coordinates with an increase of the neutron energy. This anisotropic distribution was represented by the second order quadratic polynomial on  $\mu$ , where  $\mu$  is a cosine of the polar angle in the C-M coordinates. The coefficients used in the polynomials were given in the O5S code.

## 2) Computational Method

Neutron histories were traced by a Monte Carlo procedure based on a random walk model in analogy to the physical process. The weight method and the expectation method with a point estimator were used in the code to improve the statistical accuracy of the calculation. Let us consider a case where a neutron injected into the medium escapes after the j-th scattering. The contribution of this neutron to the flux at the detector position is given by the equation:

$$\Phi_n(E) = \frac{1}{N} \sum_{n=1}^N \sum_{l=1}^{j_n} e^{-\Sigma_t(E) \rho d_l} f(\Omega_{l-1}, E_{l-1} \rightarrow \Omega_l, E_l) \times w_l \delta(E - E_l) \Delta \Omega_l,$$

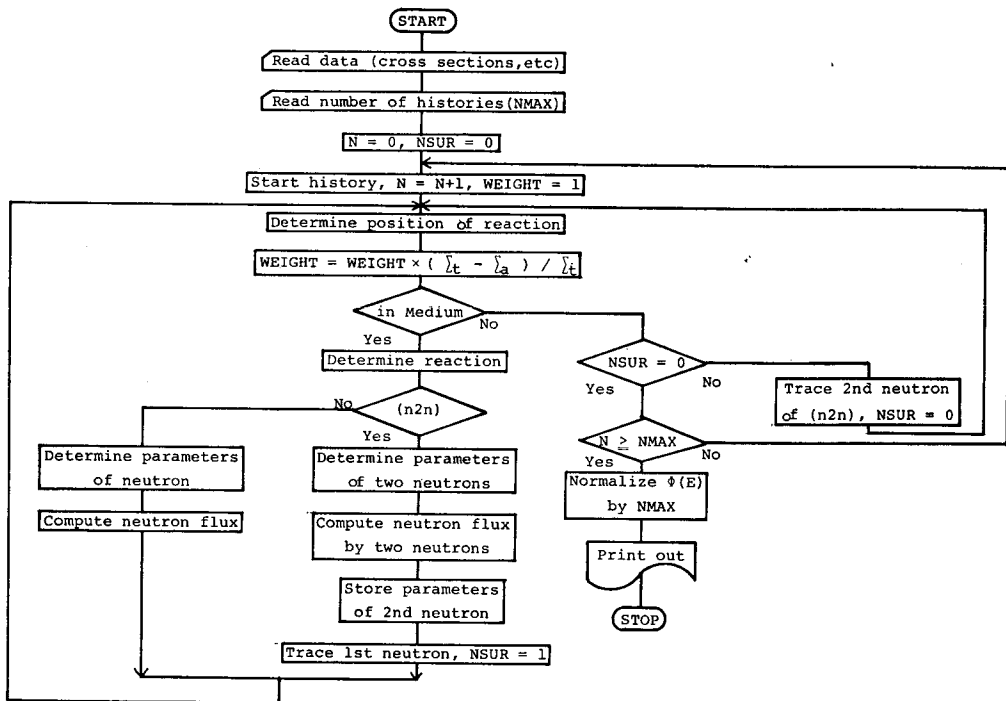


Fig. 1. Flow diagram of the Monte Carlo code.

where  $\sum_l \Sigma_l(E_l)$  = total cross section of neutron with energy  $E_l$  after the  $l$ -th collision,  
 $d_l$  = path length inside the medium of neutron scattered from the  $l$ -th collision point  $r_l$  towards the detector,  
 $f(\Omega_{l-1}, E_{l-1} \rightarrow \Omega_l, E_l)$  = total probability of neutron transfer from  $\Omega_{l-1}, E_{l-1}$  to  $\Omega_l, E_l$ ,  
 $\Delta\Omega_l$  = solid angle of the detector subtended at point  $r_l$ ,  
 $W_l$  = weight of neutron after the  $l$ -th collision,  

$$= \prod_{l'=1}^l \frac{\Sigma_l(E_{l'}) - \Sigma_a(E_{l'})}{\Sigma_l(E_{l'})},$$
 $\Sigma_a(E_{l'})$  = absorption cross section of the neutron with energy  $E_{l'}$ ,  
 $N$  = maximum number of history.

The Monte Carlo history was terminated when the neutron escaped from the medium, or its energy became lower than the cutoff energy. The flow diagram of the calculation is shown in Fig. 1.

### 3) Test Calculation

In order to check the accuracy of this code, a comparison was made with the experimental values by Hansen et al<sup>17)</sup>. They measured the leakage neutrons from the graphite shell of the thickness of 2.9 mean-free-paths, using neutrons from T(d, n) reactions

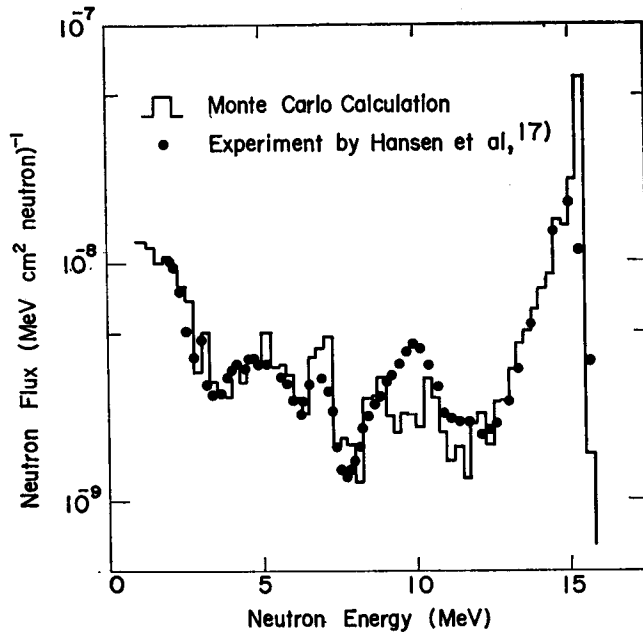


Fig. 2. Comparison of calculated and measured neutron spectra from graphite shell of 1.9 mfp in thickness for a point isotropic  $T(d, n)$  neutron source observed from 30 Deg.

which took place at the center of the shell. The calculation was carried out on the conditions given by Hansen. The results are shown in Fig. 2. They show fairly good agreement in the absolute value, except around 10 MeV. At energies around 10 MeV, the calculated value is lower than the measured value. This is caused from errors in the data of the  $(n, n')$  and  $(n, n'\alpha)$  reactions; the cross section data, the excitation functions and the angular distributions of scattered neutrons.

Previously, a graphite target was bombarded with 52-MeV protons, and measurements were carried out of secondary neutrons from the target<sup>10)</sup> and of their penetration through graphite slabs<sup>1)</sup>. Penetrating neutron fluxes were calculated with this code, using the secondary neutrons from the target as source neutrons. Calculated results agreed fairly well with the experimental spectra, and the utility of the code was confirmed.

### III. Calculation of Neutron Penetration

#### 1) Description of the Calculation

In this section, the neutron attenuation profiles in graphite and polyethylene media are studied with this code.

A geometrical arrangement for the calculation is shown in Fig. 3. The distance between the source and the detector was fixed at 1 m and the slab thickness was varied

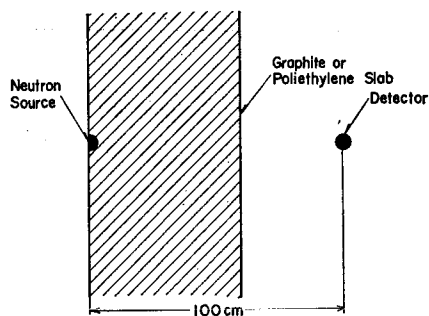


Fig. 3. Geometrical arrangement of the Monte Carlo calculation.

from 30 to 90 cm. A point source was placed at the center of the front surface of the slab. Neutrons were emitted isotropically in the forward hemisphere. Source neutron energies of 30 and 45 MeV were assumed in the calculations. The assumed atomic densities in graphite and polyethylene are shown in Table 2, where the dimensions of the slabs used in the calculations are also shown. The lower cutoff energy of the calculation was set at 50 keV.

## 2) Calculated Results and Discussion

Calculated spectra for the source energy of 30 MeV and for the slab thickness of 60 cm are shown. The numbers of the neutron histories used in the calculations were  $5 \times 10^3$  for graphite and  $5 \times 10^4$  for polyethylene. The statistical convergence of Monte Carlo calculation for graphite was achieved more rapidly than for polyethylene. This can be explained as following:

- (i) The total cross sections of polyethylene are smaller than those of graphite, so neutrons escape from the slab more easily.
- (ii) Hydrogen contained in the polyethylene slows neutrons rapidly down below the cutoff energy.

The required computing time was 107 sec and 205 sec on the FACOM M-190 computer for graphite and polyethylene, respectively.

In the graphite spectrum, there is a peak at the energy interval 27–28 MeV, just below a larger peak at 30 MeV. The latter corresponds to the uncollided neutrons or

Table 2. Dimensions and Physical Properties of Slabs.

Material	Slab Thickness (cm)	Density (g/cm <sup>3</sup> )	Atomic density (atom/cm <sup>3</sup> )	
			Carbon	Hydrogen
Graphite	30, 60, 90	1.68	8.4(+22)*	—
Polyethylene	30, 60, 90	0.931	4.0(+22)	8.0(+22)

\* Read as  $8.4 \times 10^{+22}$

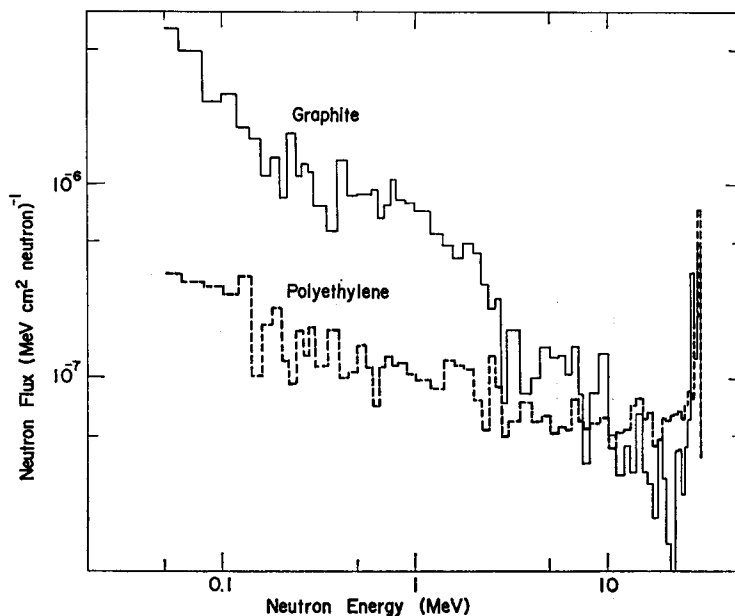


Fig. 4. Calculated neutron energy spectra transmitted through 60-cm thick graphite and polyethylene injected into 30-MeV neutrons.

to the elastically scattered neutrons at small angles. In contrast to this, the former peak has no physical meaning, because it corresponds to a small peak caused by the distortion in the differential scattering cross section due to the truncation of the Legendre expansion at the sixth order. Due to this effect, similar peak and negative fluxes appeared in all graphite spectra for 45 MeV. The angular distribution of the elastically scattered neutrons by the carbon nucleus becomes very strongly peaked in the forward direction at energies higher than 20 MeV. This means that neutron direction and energy are scarce-

Table 3. Neutron Attenuation Coefficients of 30- and 45-MeV Energies in Graphite and Polyethylene Slabs.

Material	Graphite ( $\rho=1.68 \text{ g/cm}^3$ )		Polyethylene ( $\rho=0.931 \text{ g/cm}^3$ )	
	Neutron Energy		Neutron Energy	
	30 MeV ( $\text{cm}^2/\text{g}$ )	45 MeV ( $\text{cm}^{-1}$ )	30 MeV ( $\text{cm}^2/\text{g}$ )	45 MeV ( $\text{cm}^{-1}$ )
For Flux ( $\geq 50 \text{ keV}$ )	2.24(-2)**3.76(-2)	1.32(-2) 2.22(-2)	4.06(-2) 3.78(-2)	2.78(-2) 2.59(-2)
For Dose ( $\geq 50 \text{ keV}$ )	2.32(-2) 3.90(-2)	1.43(-2) 2.40(-2)	4.04(-2) 3.76(-2)	2.82(-2) 2.63(-2)
$\Sigma_{\text{nonel.}}^*$	2.27(-2) 3.81(-2)	1.68(-2) 2.83(-2)	1.96(-2) 1.82(-2)	1.45(-2) 1.35(-2)

\* The nonelastic cross section data were cited from the O5S library data set<sup>13)</sup> for reference.

\*\* Read as  $2.24 \times 10^{-2}$



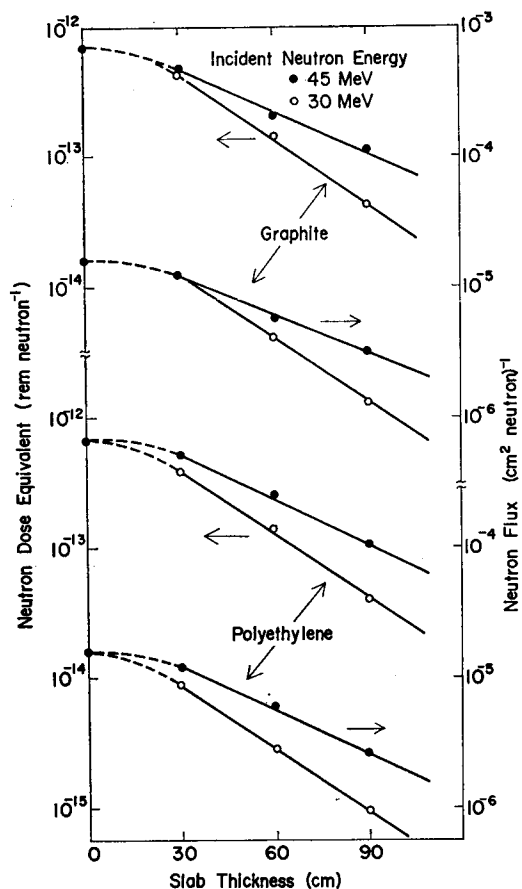


Fig. 5. Attenuation of calculated neutron fluence ( $\geq 50$  keV) and dose equivalent ( $\geq 50$  keV) as a function of graphite and polyethylene thicknesses for 30- and 45-MeV neutrons.

ly changed by this reaction, so the elastic scattering with a carbon nucleus can be omitted from the Monte Carlo calculation. The calculations were repeated, omitting this reaction in the energy range higher than 20 MeV. The obtained dose equivalent agreed well with that obtained with the elastic scattering with an accuracy of 10% in the worst case. There was no more oscillation in the spectrum, and the running time was reduced to about half. This method is one of the useful ways for handling high-energy neutrons.

The attenuation profiles of dose equivalents and total fluxes above 50 keV obtained with the elastic scattering are shown in Fig. 5. The removal cross sections determined from the attenuation profiles in the figure are given in Table 3. It may be possible from the figure and the table to say that

- (i) The attenuation curves of flux and dose equivalents are very close together both for graphite and polyethylene.

- (ii) The removal cross sections of graphite and polyethylene are also close together for 30 and 45 MeV in the cm unit.
- (iii) The removal cross sections for graphite are in good agreement with the non-elastic cross sections for 30 and 45 MeV, but not for polyethylene. This indicates that the removal cross section becomes close to the non-elastic cross section for the higher energy regions of 30 and 45 MeV in non-hydrogeneous media.

#### IV. Summary

Neutron penetration through graphite and polyethylene was studied, using the new Monte Carlo code, whose accuracy was checked with the experimental values. The attenuation profiles of 30 and 45 MeV mono-energetic neutrons through graphite and polyethylene slabs were obtained. From the profiles, the removal cross sections were calculated. The removal cross sections are very close together for both media. The removal cross section for graphite becomes close to the non-elastic cross section in the higher energy region.

#### Acknowledgement

The authors are grateful to Dr. T. Nakamura for his very useful advice about the experiment and the calculation. Also the authors are grateful to Messers. K. Hayashi and T. Saito for their helpful assistance during the experiment.

#### References

- 1) K. Shin, Y. Uwamino, M. Yoshida, T. Hyodo and T. Nakamura; submitted to Nucl. Sci. Eng.
- 2) R. G. Alsmiller, Jr., R. T. Santoro and J. Barish; Trans. Amer. Nucl. Soc., **21**, 546 (1975).
- 3) W. W. Wadman III; Nucl. Sci. Eng., **35**, 220 (1969).
- 4) J. P. Meulders, P. Leleux, P. C. Macq, C. Pirart and G. Valenduc; Nucl. Instr. Methods, **126**, 81 (1975).
- 5) R. G. Alsmiller, Jr., F. R. Mynatt, J. Barish and W. W. Engle, Jr.; Nucl. Sci. Eng., **36**, 251 (1969).
- 6) R. G. Alsmiller, Jr., F. R. Mynatt, J. Barish and W. W. Engle, Jr.; Nucl. Instr. Methods, **72**, 213 (1969).
- 7) R. G. Alsmiller, Jr., F. R. Mynatt, M. L. Gritzner, J. V. Pace and J. Barish; Nucl. Instr. Methods, **89**, 53 (1970).
- 8) R. G. Alsmiller, Jr., M. Leimdörfer and J. Barish; "Analytic representation of nonelastic cross sections and particle-emission spectra from nucleon-nucleus collisions in the energy range 25 to 400 MeV"; *ORNL-4046*, Oak Ridge National Laboratory (1967).
- 9) H. W. Bertini; "Monte Carlo calculations on intranuclear cascades"; *ORNL-3383*, Oak Ridge National Laboratory, (1963).
- 10) T. Nakamura, M. Yoshida and K. Shin; Nucl. Instr. Methods, **151**, 493 (1978).
- 11) A. Fasso and M. Höfert; Nucl. Instr. Methods, **133**, 213 (1976).
- 12) H. Hirayama and T. Nakamura; Mem. Fac. Eng., Kyoto Univ., **33**, 187 (1972).
- 13) R. E. Textor and V. V. Verbinski; "O5S: A Monte Carlo code for calculating pulse height distributions due to monoenergetic neutrons incident on organic scintillators", *ORNL-4160*, Oak Ridge National Laboratory (1968).

- 14) I. Langner, J. J. Schnidt and D. Wall; "Tables of evaluated nuclear cross sections for reactor materials", *KFK-750*, EUR-3715e EANDC(E)-88 "U", Kernforschungszentrum, Karlsruhe (1968).
- 15) S. K. Penny, W. E. Kinney and F. G. Pery; *ENDF/B-III* Material 1165, Brookhaven National Laboratory.
- 16) D. C. Iruing et al.; "O5R: A general-purpose Monte Carlo neutron transport code", *ORNL-3622*, Oak Ridge National Laboratory (1965).
- 17) L. F. Hansen, C. Wong, T. Komoto and J. D. Anderson; *Nucl. Sci. Eng.*, **60**, 27 (1976).